Journal of Applied Polymer Science

Preparation, Morphology, and Conductivity of Waterborne, Nanostructured, Cationic Polyurethane/Polypyrrole Conductive Coatings

Haihua Wang, Yun Liu, Guiqiang Fei, Jing Lan
Key Laboratory of Auxiliary Chemistry & Technology for Chemical Industry, Ministry of Education, Shaanxi University of Science & Technology, Xi'an, Shaanxi 710021, China
Correspondence to: H. Wang (E-mail: wseaflower@126.com)

ABSTRACT: To endow cellulose fiber papers with good conductivity and simultaneously retain the mechanical strength of the conductive paper, a kind of waterborne, nanostructured, cationic polyurethane (CPU)/polypyrrole (PPy) conductive coatings were developed to modify the paper surface. Fourier transform infrared spectroscopy, atomic force microscopy, and thermogravimetry–differential thermogravimetry demonstrated that the peak associated with hydrogen bonding between —NH and C═O of CPU was shifted, and chemical bonds between CPU and PPy were formed. Good compatibility between CPU and PPy was simultaneously established. Transmission electron microscopy and atomic force microscopy also suggested that PPy was encased and embedded in the CPU colloidal particles in a uniform style, and the surface of the CPU/PPy film was covered with a smooth, coherent conductive layer. With increasing pyrrole (Py) content from 5 to 20 wt %, the particle size increased from 55.08 to 74.59 nm, and the dispersity index (DPI) decreased. In addition, the conductivity of CPU/PPy increased from 0.1 to 5.0 S/cm. When the Py content was greater than 20 wt %, apparent increases in the particle size and DPI were detected as was particle coagulation; this resulted in decreased conductivity. Compared with the uncoated paper, the paper coated with CPU/PPy dispersions displayed different surface morphologies. The surface of the paper was completely enwrapped by the CPU/PPy conductive films when the coating amount was 45.42 g/m^2. With increasing coating amounts from 10.35 to 67.86 g/m^2, the conductivity of the conductive coated paper increased from 2.78×10^{-3} to 2.16 S/cm, the tensile strength increased from 35.3 to 60.4 N m/g, and the conductive coated paper displayed good conductivity stability. © 2014 Wiley Periodicals, Inc. J. Appl. Polym. Sci. **2015**, *132*, 41445.

KEYWORDS: cellulose and other wood products; coatings; conducting polymers; polyurethanes; properties and characterization

Received 18 June 2014; accepted 25 August 2014
DOI: 10.1002/app.41445

INTRODUCTION

Nowadays, the coating of cellulose fiber papers with conducting polymers has drawn great attention in the form of new functional papers and packaging applications, such as antistatic and electromagnetic shielding papers, novel wall coverings, electrical resistive heating papers, and antibacterial papers.[1,2] Among the known conductive polymers used for coating conductive papers, polypyrrole (PPy) is one of the most extensively studied because of its high electrical conductivity, good stability, heterocyclic structure, and nontoxicity.[3,4] Heretofore, the *in situ* chemical oxidative polymerization of pyrrole (Py) monomer on individual cellulose fibers is the most popular method for preparing conductive cellulose fibers.[3–6] The conductive paper sheets made from such conductive-polymer-encapsulated fibers display a decreased tensile strength; this can be contributed to the acid hydrolysis and oxidative degradation of the fibers during the *in situ* chemical oxidative polymerization.[3,7] In addition, the presence of PPy clusters on the fiber surface decreases the interfiber hydrogen bonding; it is also responsible for the decrease in the tensile strength of the conductive paper.[3,7] Under such circumstances, the preparation of a conductive cellulose fiber paper through the application of a conductive polymer on the surface of the paper is put forward in this article.

Waterborne polyurethane (WPU) exhibits several advantageous properties, including a good abrasion resistance, flexibility, impact resistance, chemical resistance, and weatherability coupled with low volatile organic compound (VOC) emission.[8] Recently, WPU has been used as a kind of surface-sizing agent in the papermaking industry.[9,10] Guo et al.[10] found that the water resistance and mechanical properties of paper sheets sized with WPU were much better than those of unsized paper sheets. Composite conductive materials based on polyurethane (PU) with conducting polymers are promising materials for many technological

applications because of their chemical versatility, stability, and processability.[11,12] These composites have been applied in the fields of antistatic materials; the corrosion protection of metals, sensors, and electromagnetic shielding; and so on.[13] At present, PU/PPy composites have been prepared by physical blending, electrochemical polymerization, and chemical polymerization.[14–17] For instance, Robilă et al.[16] prepared conductive PU/PPy composites by immersing the anode coated by the PU film in a solution containing both electrolyte and Py. Kotal et al.[18] prepared a thermoplastic PU/PPy nanoblend in tetrahydrofuran by a solution-blending process and an *in situ* process. Large amounts of organic solvent are used in the aforementioned process. However, the increasing demands to reduce volatile organic compounds and hazardous air pollutants have led to increased efforts to formulate waterborne conductive PUs.

The combination of polymer latexes and conducting polymers has been demonstrated to produce waterborne conductive dispersion with new and unique properties.[17] However, the simple mixing of a conducting polymer with a latex can hardly yield homogeneous conductive composites,[17] and phase separation is easily generated.[18] The *in situ* surface modification of a latex with a conducting polymer has been demonstrated to be a good method of choice when the latex is stabilized.[17] In general, colloidal particles are able to be colloidally stable on the basis of the introduction of the polymeric stabilizer to the latex,[17] such as poly(*N*-vinyl pyrrolidone) (PVP),[17,19,20] poly(vinyl alcohol),[21] or hydroxypropylcellulose.[22] However, most reports have focused on the preparation and properties of PU/polyaniline latexes.[23] Just a few reports are available on the utilization of PPy for the preparation of waterborne conductive PU composites.[24] Wiersma et al.[24] obtained core–shell PPy/PU dispersions by simultaneously adding $Fe(NO_3)_2$ and Py to a commercial nonionic PU dispersion, and the conductive coating was used as a textile coating. However, the effects of the structural characteristics of PU, the preparation procedure on the properties of the PU/PPy dispersions, and the corresponding conductive films are still ambiguous. None of these preparations have used waterborne cationic polyurethane (CPU) as a dopant and template in the development of waterborne conductive coatings. It was reported that the presence of ionic groups in PU was able to produce a significant increase in the elecroconductive polymer ratio in conductive composites. Also, the higher hydrophilic nature of PU ionomers provides a more favorable environment for the diffusion of Py and $FeCl_3$ aqueous solutions.[25]

In our previous work,[26] a series of waterborne CPU/PPy dispersions was prepared through the addition of oxidant and Py to a CPU dispersion, and the effects of the Py content, reaction temperature, reaction time, and molar ratio of oxidant to Py on the surface resistivity of the conductive films were systematically investigated. However, to further improve the compatibility between PPy and PU, Py was introduced into the reaction system to react with the isocyanate (NCO)-terminated PU prepolymer, and then, water was added to obtain WPU/PPy dispersions. Furthermore, the utilization of the waterborne conductive CPU dispersion as a conductive coating for cellulose fiber paper sheets was not discussed.

The main objective of this study was to combine the merits of WPU and conductive PPy to develop an efficient waterborne, nanostructured, conductive coating for cellulose fiber papers. In addition to endowing the papers with conductivity, the coated paper was also expected to retain its mechanical strength. In this study, a series of waterborne nanostructured CPU/PPy dispersions with good compatibility were prepared. The structure, morphology, mechanism, phase behavior, and electrical conductivity of the CPU/PPy dispersions and corresponding films were systematically investigated as were their morphology, tensile strength, surface resistivity, and conductivity stability of the conductive paper coated with CPU/PPy.

EXPERIMENTAL

Materials

Py (Enterprise Group Chemical Reagent Co., Ltd.) was vacuum-distilled before use. Poly(ethylene glycol) (PEG; number-average molecular weight = 2000, Tianjing Chemical Reagent Factory) was dried and degassed at 100°C under 1–2 mmHg for 2 h before synthesis. Isophorone diisocyanate (IPDI; Germany Bayer Corp.) and *N*-methyl diethanol amine (MDEA; Shanghai Haohua chemical Co., Ltd.) were used as received. Acetic acid glacial (CH_3COOH), ferric chloride ($FeCl_3$), *N*-methyl pyrrole, and HCl were purchased from Tianjing Chemical Reagent Factory and were used as received. The staining agent, phosphotungstic acid, was purchased from Shanghai Yuanmo Bio-Technique Co., Ltd., and was used as received.

Preparation of Waterborne Cationic Nanostructured PU/PPy Dispersions

A calculated amount of IPDI (0.03 mol), *N*-methyl pyrrole, PEG 2000 (0.01 mol), MDEA (0.016 mol), and dibutyl dilaurate (DBTDL) were charged into a three-necked flask equipped with a stirrer, reflux condenser, and nitrogen purge. The reaction mixture was heated to 70°C and stirred for 3 h to prepare the NCO-terminated PU prepolymer. Then, Py's with different contents (on the basis of the weight of the PU prepolymer) were added to the reaction systems. After 1 h, the reaction mixture was then cooled to 30°C, and CH_3COOH (0.032 mol) was added and stirred for another 0.5 h. Then, water was added under vigorous stirring to produce the waterborne CPU/Py dispersions.

Then, an $FeCl_3$ solution with a concentration of 40 wt % was introduced into the flask to adjust the pH value to 2. The chemical oxidation reaction was kept going for another 1 h to obtain the waterborne, cationic, nanostructured PU/PPy (CPU/PPy) dispersions. The preparation procedure and structure of CPU/PPy are shown in Figure 1. The samples were designated as CPU/PPy-5, CPU/PPy-10, CPU/PPy-15, CPU/PPy-20, CPU/PPy-25, and CPU/PPy-30. The number 5 indicates that the PPy content was 5 wt % on the basis of pure CPU; the others were the same. The low-molecular-weight compounds were removed by exhaustive dialysis in a dialysis bag against 0.2*M* HCl.

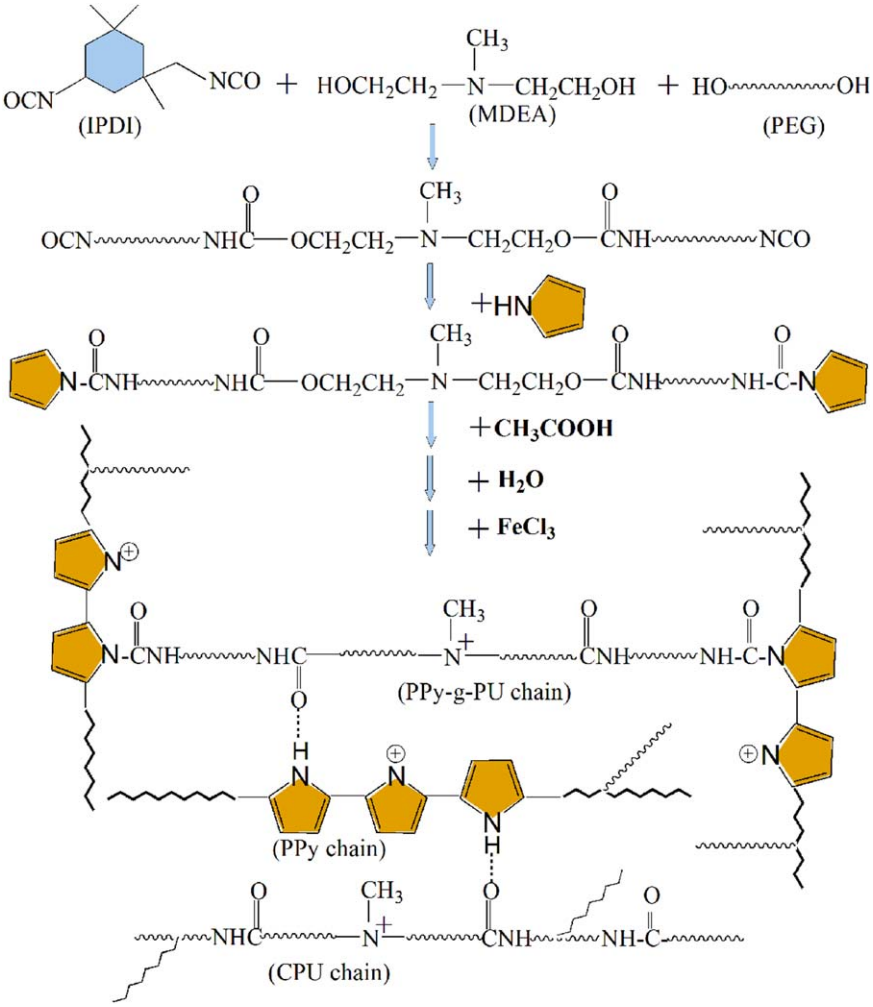

Figure 1. Preparation of the cationic WPU/PPy dispersion. [Color figure can be viewed in the online issue, which is available at www.interscience.wiley.com.]

Preparation of the CPU/PPy Films

The CPU/PPy films were prepared by spin coating on a freshly cleaved glass plate for the measurement of the surface morphology and surface resistivity.

Preparation of the Conductive Coated Paper

A 30 × 30 cm^2 cellulose fiber paper sheet was placed on the working plate of an ST-1–260 coater (Shaanxi University of Science and Technology, China). Before coating, the paper sheet was firmly pressed on the working plate to prevent any folding or curling and was then fixed. Next, the CPU/PPy dispersion was poured onto the paper sheet, and a coating roller was used at a constant rate of 3.0–4.0 mm/s to obtain a uniformly coated conductive paper. The coated paper sheet was dried for 48 h at room temperature. For each kind of CPU/PPy dispersion, five paper sheets were obtained. The conductive coated paper sheets were conditioned at 23 ± 1°C and 50 ± 2% relative humidity for 24 h before characterization.

Characterization

Fourier transform infrared (FTIR) spectroscopy spectra of the samples were recorded on an FTIR spectrometer (Bruker Optics Vector-22, Germany) with KBr pellets at frequencies of 4000 to 400 cm^{-1} at a 1-cm^{-1} resolution, signal-averaged over 32 scans, and baseline-corrected.

The ^{1}H-NMR and ^{13}C-NMR spectra of the CPU prepolymer and CPU/Py prepolymer were determined by NMR (Bruker Avance 400 MHz, Germany). *D*-Substituted dimethyl sulfoxide was used as a solvent, and tetramethylsilane was used as the internal standard.

The particle size and distribution values of the CPU and CPU/PPy dispersions were analyzed by dynamic light scattering (Malvern Zetasizer Nano-ZS ZEN 3500, United Kingdom). The morphologies of the CPU and CPU/PPy colloidal particles were observed by transmission electron microscopy (TEM; Hitachi S570, Japan) with phosphotungstic acid as a staining agent.

The morphologies of the surfaces of the CPU/PPy films were studied with atomic force microscopy (AFM; Seiko SAC400-SPI3800N, Japan). All measurements were made in contact mode.

The surface resistivity of the CPU/PPy films and conductive coated papers was determined with a four-point van der Pauw method with a Keithley 237 high-voltage source and a Keithley

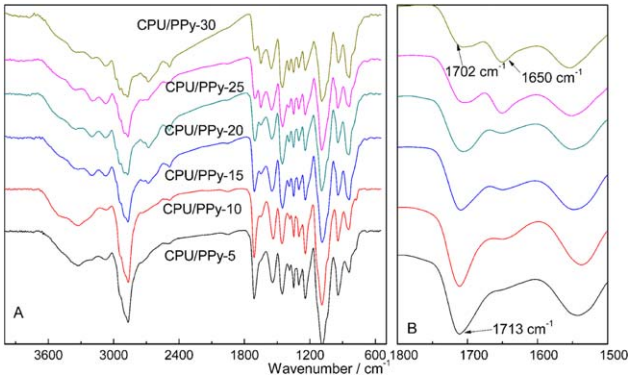

Figure 2. FTIR spectra of CPU/PPy coatings with different Py contents. [Color figure can be viewed in the online issue, which is available at www.interscience.wiley.com.]

2010 multimeter. The surface resistivity was measured by a standard four-probe method.

Thermal analysis of the samples was performed on a thermogravimetric analyzer (Q500) under a nitrogen atmosphere in the temperature range of 30–550°C with a heating rate of 15°C/min.

The tensile strength of the uncoated and coated paper sheets were evaluated on a TS2000-S universal testing machine (Scientific and Technological Limited Co., High Iron, Taiwan) with a sample width of 25 mm and an initial sample length of 180 mm. The measurements were repeated at least five times.

The surface morphologies of the uncoated and coated paper sheets were observed with an environmental scanning electron microscope (SEM, Hitachi S-4800, Japan). All of the samples were coated with gold *in vacuo* before SEM observation.

RESULTS AND DISCUSSION

Structural Analysis

The FTIR spectra of the CPU/PPy with different Py contents are shown in Figure 2. The characteristic peaks of the urethane group were observed at 3337 and 1714 cm^{-1}; these corresponded to the stretching vibrations of hydrogen-bonded —NH and C═O groups, respectively. This suggested the presence of hydrogen-bonding interactions between the —NH and C═O groups of CPU.[13] It was found that significant shifts took place in the characteristic peaks of the —NH and C═O groups, as shown in the FTIR spectra. The intensities of the —NH and C═O peaks decreased with increasing Py content, and the peak at 1713 cm^{-1} redshifted to 1702 cm^{-1}. Meanwhile, a new peak at 1650 cm^{-1} corresponding to the C═O of urea appeared, and the intensity became more pronounced with increasing Py content. This certified the reaction between CPU and PPy. The increasing ratio of the intensity of the band at 1650 cm^{-1} to that of the band at 1713 cm^{-1} (I_{1650}/I_{1713}, I represents Intensity) also suggested relatively more site-specific interactions between CPU and PPy with increasing Py content,[18,27] and the hydrogen-bonding interactions between the —NH and C═O groups of CPU were simultaneously weakened. The schematic representation of the CPU/PPy networks is shown in Figure 1.

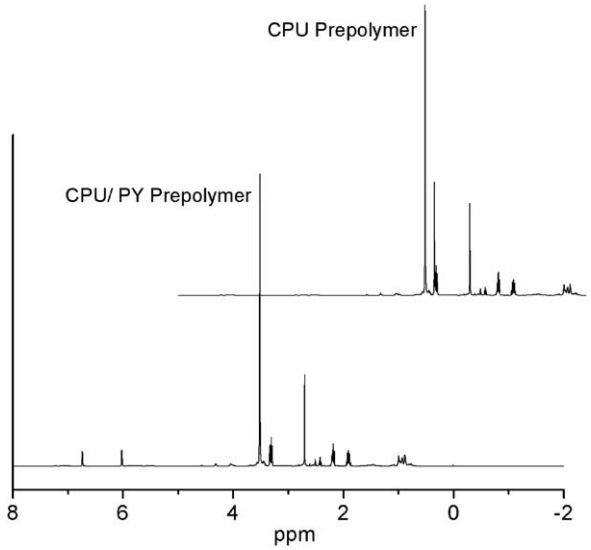

Figure 3. ^{1}H-NMR spectra of the CPU and CPU/Py prepolymers.

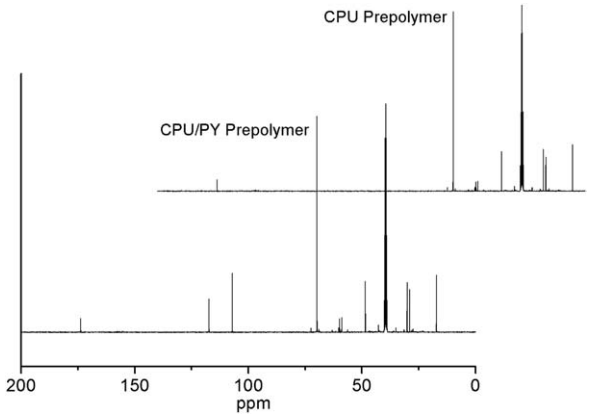

Figure 4. ^{13}C-NMR spectra of the CPU and CPU/Py prepolymers.

The peaks at about 1539 and 1457 cm^{-1} were due to the C═C and C—N stretching in the Py ring, respectively;[28] this also supported evidence for the successful incorporation of PPy into the CPU matrix. We found that the ratio of the intensity of the symmetric mode at 1457 cm^{-1}(A2) to the intensity of the antisymmetric ring stretching mode at 1539 cm^{-1}(A1) increased with increasing PPy content. We concluded that PPy with a longer conjugation length was obtained at higher Py contents and resulted in a higher conductivity.[29] In addition, the peak at 1295 cm^{-1} represented the presence of C—N in-plane deformation vibrations.[30] The observed sharp bands at 1045 and 776 cm^{-1} were due to the C—H in-plane deformation and out-of-plane stretching, respectively.

The ^{1}H-NMR spectra of the CPU prepolymer and CPU/Py prepolymer are presented in Figure 3. As shown in Figure 3, signals observed in the region from 3.29 to 4.04 ppm belonged to the proton of —CH_2—O—. The signals ranging from 1.87 to 1.95 ppm were ascribed to the proton of —CH_2.[31] The signals at 2.70 ppm were attributed to the proton of —NCH_3. Compared to the ^{1}H-NMR spectrum of the CPU prepolymer, new signals were detected in the ^{1}H-NMR spectrum of the CPU/Py

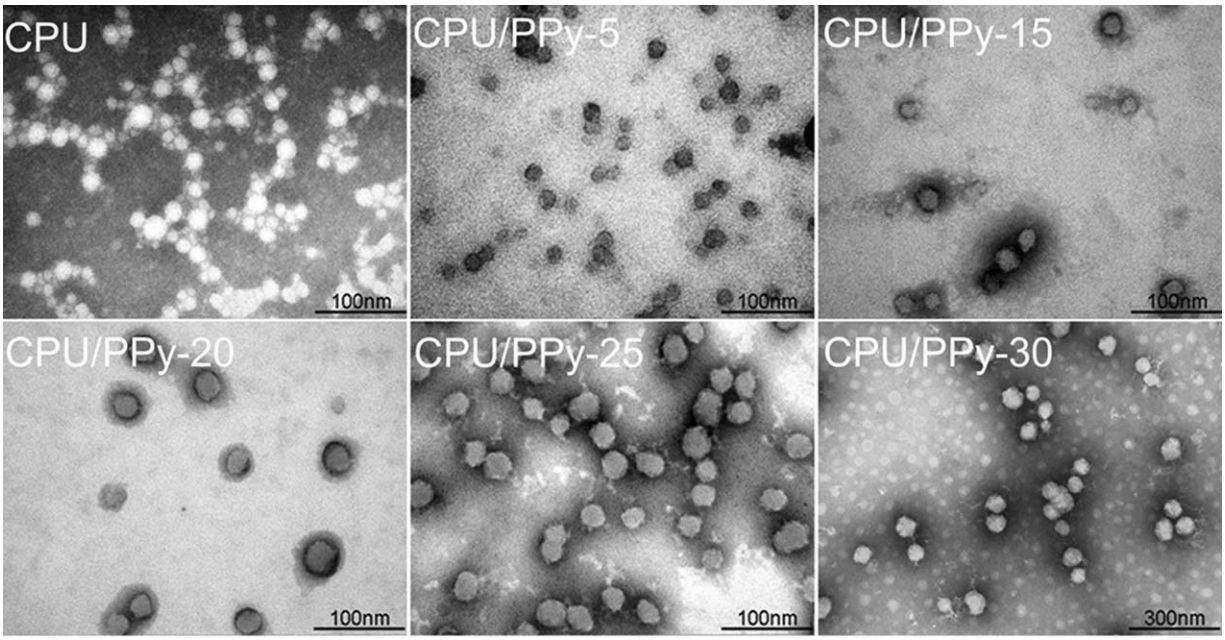

Figure 5. TEM images of the nanostructured CPU and CPU/PPy dispersions with different Py contents.

prepolymer. The signals at 6.74 and 6.02 ppm were assigned to the α-H and β-H of the Py rings.[32]

The ^{13}C-NMR spectra of the CPU prepolymer and CPU/Py prepolymer are shown in Figure 4. As shown in Figure 4, the signals at 173.72 ppm belonged to the carbon atom of —NH*C*OO—. Carbon atom of —COO*C*H_2— were detected at 69.76 ppm. The signals observed at 48.45 ppm belonged to the carbon atom of —*C*H_2N—. The chemical shift at 27.45–31.50 ppm confirmed the carbon atom of —CH_2—. The signals observed at 17.19 ppm were ascribed to the carbon atom of —CH_3.[33] Two new peaks at 117.29 and 107.03 ppm were attributed to the α-C and β-C of the Py rings.[34] The reaction between CPU and PPy was further confirmed by the aforementioned results.

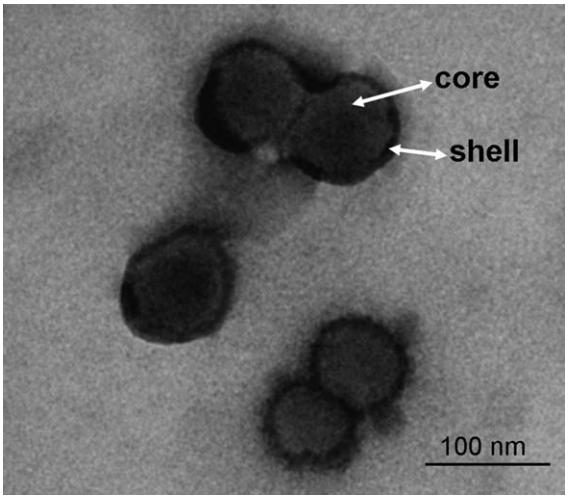

Figure 6. TEM morphology of the CPU/PPy-20 colloidal particles at high magnification.

Morphological Analysis

In the process of preparing conductive PU dispersions, Py is generally introduced directly into the PU dispersion. It is easy for hydrophobic Py and PPy oligomers to anchor onto the colloidal particles; this results in the deposition of PPy on the surface of colloidal particles, and the colloidal nature of the substrate is preserved.[17,22] In general, a composite precipitate of micrometer-sized particles is often obtained when PU dispersion on a nanosized level is adopted.[17,31] Therefore, water-soluble polymeric stabilizers are used to prevent the macroscopic precipitation of conducting polymers.[17] It was reported by Chen and Liu[35] that micrometer-sized particles of large polydispersity in size were obtained for PU/polyaniline composites in the absence of PVP and displayed a coral-like morphology. The particle size and polydispersity were reduced with the addition of PVP, and particles of good dispersity were obtained.[17] However, stable CPU/PPy dispersions with nanosized particles and narrow particle size distributions were obtained when no polymeric stabilizer was used in this study.

The TEM images of the CPU and CPU/PPy colloidal particles prepared with different Py contents are shown in Figure 5. In this study, the CPU and CPU/PPy colloidal particles for TEM testing were obtained through negative staining with phosphotungstic acid. The darker phase in the TEM image of CPU was ascribed to the higher electronic cloud density on the out layer of the CPU colloidal particles. The CPU colloidal particles presented a heterogeneous distribution, and significant aggregations among CPU colloidal particles were also detected in the TEM image of the CPU dispersion. With the incorporation of the cationic PPy into the PU backbone, the electronic cloud density inside the colloidal particles became higher, and the CPU/PPy-5 colloidal particles showed a relative uniform morphology. The particles dispersed with each other because of stronger static exclusion with the introduction of PPy. In addition, smaller

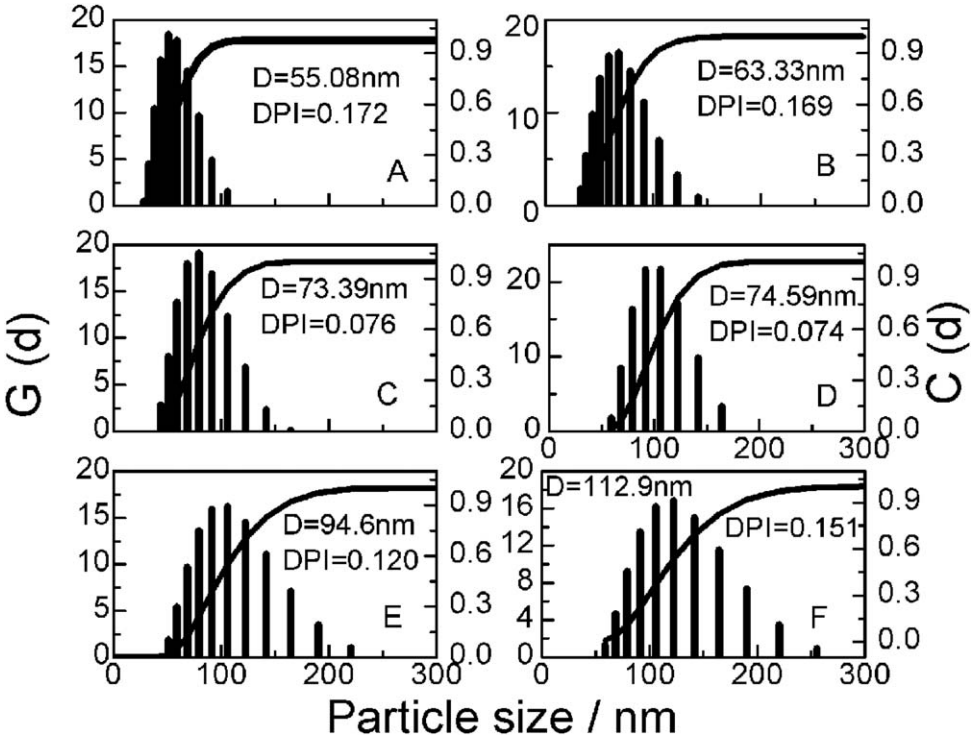

Figure 7. *D* and distribution values of the CPU and CPU/PPy dispersions: (A) CPU/PPy-5, (B) CPU/PPy-10, (C) CPU/PPy-15, (D) CPU/PPy-20, (E) CPU/PPy-25, and (F) CPU/PPy-30. G represents weight percentage; C represents comulants.

particles with more uniform and globular shapes were obtained for the CPU/PPy dispersion with 5 wt % Py addition. This might have been due to the good compatibility and strong interactions between the PPy and CPU chains. This indicated that the PPy chains were distributed uniformly inside the CPU colloidal particles. With increasing Py content from 5 to 20 wt %, the particle size increased, and the contrast between the core and shell part became more distinguishable, as shown in Figures

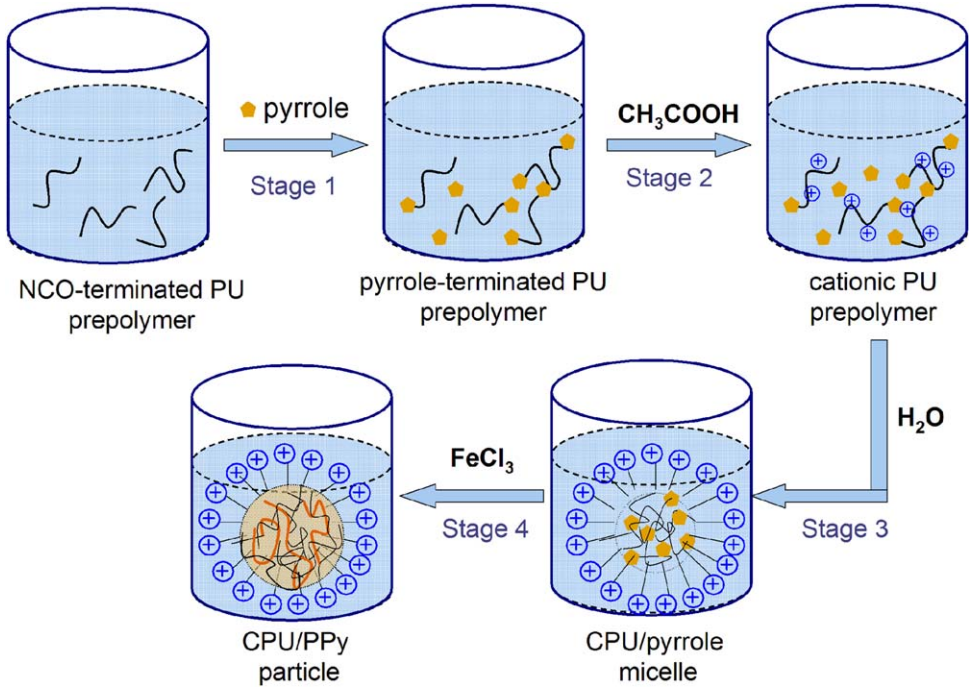

Figure 8. Schematic illustration of the mechanism for the formation and stability of the CPU/PPy dispersions. [Color figure can be viewed in the online issue, which is available at www.interscience.wiley.com.]

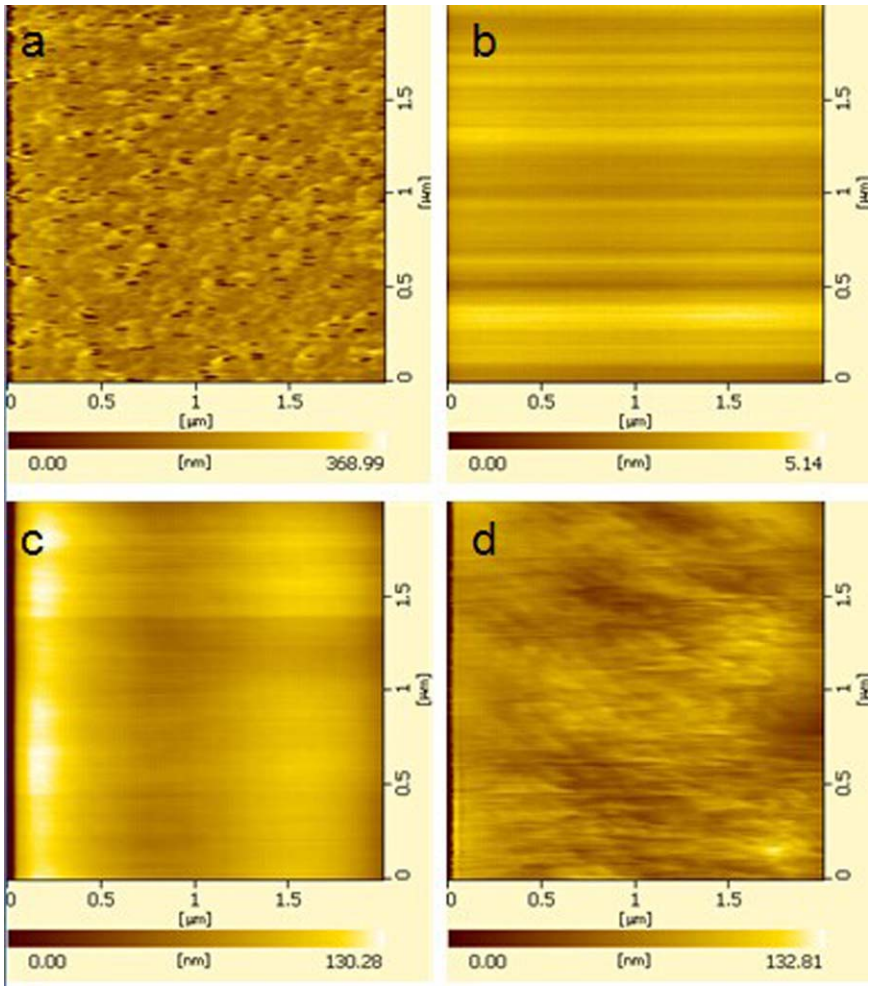

Figure 9. AFM phase images of the CPU and CPU/PPy films: (a) CPU, (b) CPU/PPy-10, (c) CPU/PPy-20, and (d) CPU/PPy-30. [Color figure can be viewed in the online issue, which is available at www.interscience.wiley.com.]

5 and 6. The gray phase is the CPU/PPy phase, whereas the darker phase is the PPy phase. The figures suggest that more and more PPy polymers were obtained with increasing Py content.

However, more and more hydrophobic PPy chains were formed with further increases in the Py content. The content of ionic groups in the CPU chains was insufficient to keep the CPU/PPy dispersion stable, and this resulted in coagulation. As shown in the TEM image of CPU/PPy-30, two kinds of particles were detected. Under such circumstances, the system lost colloidal stability, and a composite precipitate of the conducting polymer was obtained.

Particle Size and Distribution Analysis

Figure 7 shows the average particle diameter (D) and dispersity index (DPI) values of the CPU and CPU/PPy dispersions determined by the light scattering technique. We found that a stable diameter curve was difficult to produce for the CPU dispersion. This might have been due to the fact that when there were too many hydrophilic groups, PU changed from a state such as a micelle to the verge of a solution state. A similar phenomenon was also observed by Chai et al.[36] for a PU dispersion when the amount of hydrophilic chain extender dimethylolpropionic acid (DMPA) was 9.9 wt %. Therefore, the D curve for the CPU dispersion is not provided in this article. The D value of the CPU/PPy dispersions increased gradually from 55.08 to 74.59 nm with increasing PPy content from 5 to 20 wt %, and DPI decreased from 0.172 to 0.074. The TEM images also showed that the CPU/PPy colloidal particles had a narrower distribution, and a mixture of two separate types of particles was not found. This indicated good compatibility between CPU and PPy. With further increases in the PPy content, a great increase in DPI was detected as was the increased D; this was attributed to the coagulation of colloidal particles, as discussed in the TEM section.

Formation and Stability Mechanism of the CPU/PPy Dispersions

On the basis of the TEM and dynamic light scattering results, a possible formation mechanism and stability mechanism of the CPU/PPy dispersions are proposed, as illustrated in Figure 8. After the preparation of the NCO-terminated PU prepolymer, Py was added and reacted with —NCO groups to produce the Py-terminated PU prepolymer, as shown in stage 1. Then,

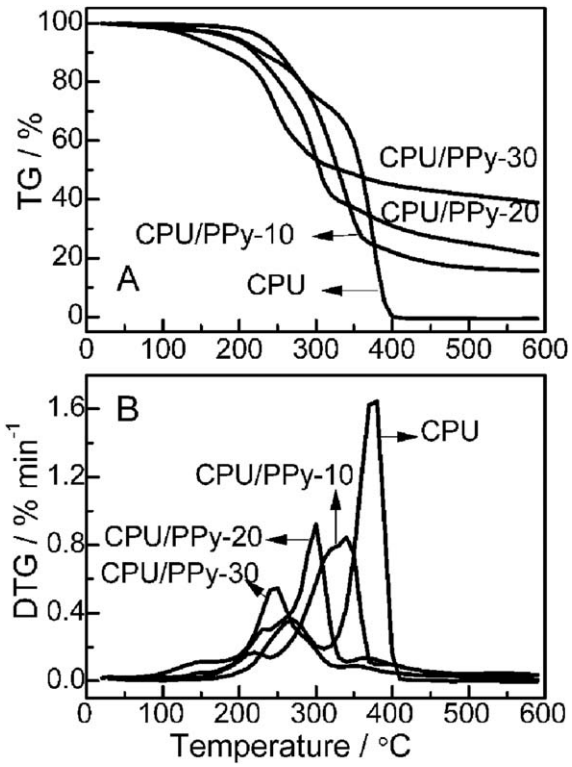

Figure 10. TG and DTG thermograms of CPU and CPU/PPy with different PPy contents.

CH_3COOH was introduced to neutralize the PU prepolymer to get the CPU/Py chain, as shown in stage 2. Afterward, water was added to make the CPU/Py self-emulsify, and CPU/Py micelles were thereby obtained. To retain the colloidal stability, hydrophilic moieties tend to be located on the surface of particles, and hydrophobic units tend to be located in the inner space of the particles.[37] Therefore, cationic groups aggregated on the surface of the CPU/Py micelles to retain the colloidal stability, as illustrated in stage 3. Finally, $FeCl_3$ was introduced to initiate the oxidative polymerization of Py, and CPU/PPy particles were thereby formed.

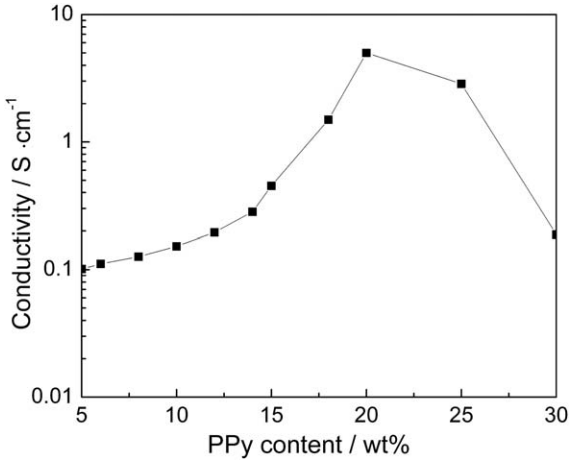

Figure 11. Variation of the conductivity of the CPU/PPy films with the PPy content.

Surface Morphology and Phase Behavior

AFM in contact mode was used to study the phase-segregated morphology of the CPU and CPU/PPy films with various PPy contents. Figure 9 shows the AFM phase portraits of the CPU and CPU/PPy films with different PPy contents. The bright aggregates, which might have been hard-segment-rich regions, were dispersed in the dark soft-segment-rich matrix for CPU.[13] The hard-segment aggregations in CPU were destroyed with the incorporation of PPy, and an ordered structure with a uniform distribution of CPU and PPy was observed for CPU/PPy-10 and CPU/PPy-20. Combined with the results from FTIR spectroscopy, TEM, and particle size distribution, this suggests that the PPy polymers were encased and embedded in the CPU colloidal particles in a uniform style, and the surfaces of CPU/PPy-10 and CPU/PPy-20 were covered with a smooth, coherent layer of electrically conductive polymer.

However, the ordered structure was destroyed when the PPy content was 30 wt %; this resulted in the particular morphology. The film cast from CPU/PPy-30 had a less regular and rougher surface; this was due to the PPy aggregation in the CPU matrix.

To further study the phase behavior of CPU/PPy, the thermogravimetry (TG) and differential thermogravimetry (DTG) thermograms of CPU and CPU/PPy with different PPy contents were also determined, as shown in Figure 10. It was apparent that CPU degraded in two stages. The first stage, at 177–310°C, corresponded to 26.51% weight loss and was due to the degradation of the hard segment in the CPU chains. The second stage, at 310–460°C, with a 72.61% weight loss was mainly attributed to the degradation of the soft segment. With the incorporation of PPy, the two aforementioned degradation peaks merged together to form a main degradation peak with shoulders at lower and higher temperatures. This suggested good compatibility and interaction between CPU and PPy. The main decomposition pattern of the CPU/PPy networks displayed a greater mass loss than that of the pure CPU. This was attributed to the lower thermal stability of the new urea-type linkages between PPy and CPU.[38]

It was also seen in the DTG curves that CPU/PPy at higher PPy contents displayed slower degradation rates and higher residue percentages. The residue percentages of CPU, CPU/PPy-5, CPU/PPy-10, CPU/PPy-20, and CPU/PPy-30 were 0, 15.61, 21.05, 38.05, and 38.73%, respectively, at 600°C. This suggested that the pyrolitic residues of PPy incorporated into PU acted as a protective barrier to improve the thermal stability of CPU/PPy.

Electrical Conductivity Analysis

Figure 11 presents the conductivity of the CPU/PPy films as a function of the PPy content. The conductivity increased from 0.1 to 5.0 S/cm with increasing PPy content from 5 to 20 wt %. It was interesting to observe that the conductivity of the CPU/PPy prepared in this study was much higher than that prepared in our previous study.[26] This could be ascribed to the relative higher compatibility between CPU and PPy. It is also worth noting that the conductivity decreased when the PPy content was greater than 25 wt %. This was attributed to the

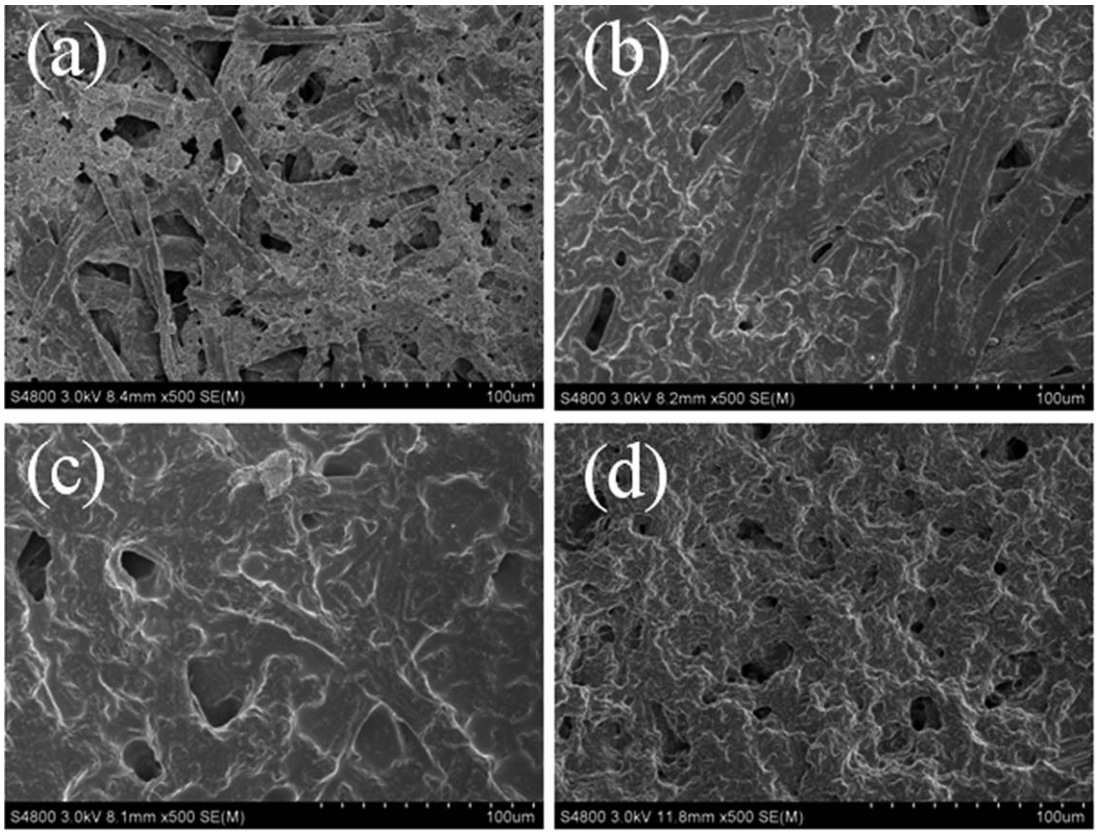

Figure 12. SEM photographs of the conductive paper surface coated with different amounts of the CPU/PPy dispersion: (a) uncoated paper, (b) paper coated with 10.35 g/m^2 CPU/PPy, (c) paper coated with 20.05 g/m^2 CPU/PPy, and (d) paper coated with 45.42 g/m^2 CPU/PPy.

heterogeneous distributed PPy aggregations in the CPU matrix, which were produced by the self-polymerization of Py.

Surface Treatment of the Paper with the CPU/PPy Dispersion

The CPU/PPy dispersion with a 20 wt % PPy content was used to coat the cellulose fiber papers. The surface morphology of the conductive paper coated with different amounts of the CPU/PPy dispersion is shown in Figure 12. For uncoated paper, bundles of cellulose fibers and pores were observed with fillers between. Compared with the uncoated paper, the paper coated with the CPU/PPy dispersion displayed a different surface morphology. For the CPU/PPy-coated paper, the polymer film was developed on the top of the fibrous substrate. With increasing coating amount, a more continuous film was formed on the surface of the conductive paper. In addition, the partial CPU/PPy coating penetrated into the paper web and warped around the fibers. In contrast, we observed a fibrous morphology when the coating amount was 45.42 g/m^2. This suggested that the surface of the conductive paper was completely enwrapped by the CPU/PPy conductive films; this was beneficial for the decrease of surface resistivity.

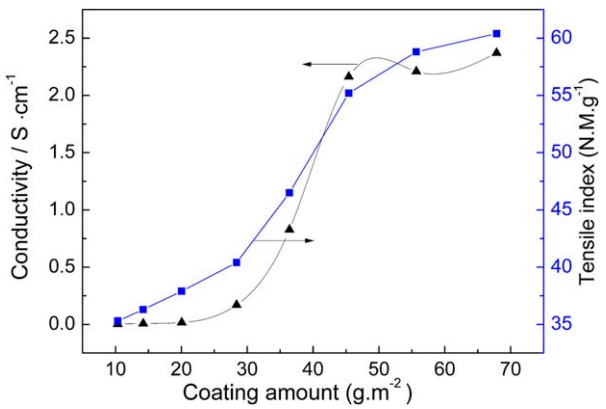

Figure 13. Effects of the coating amount on the conductivity and tensile strength of paper coated with CPU/PPy-20. [Color figure can be viewed in the online issue, which is available at www.interscience.wiley.com.]

Figure 13 shows the effects of the coating amount on the conductivity and conductive stability of the conductive paper coated with the CPU/PPy dispersion. With increasing coating amount from 10.35 to 45.42 g/m^2, the conductivity increased abruptly from 2.78 $\times$ 10^{-3} to 2.16 S/cm. The conductivity began to level off when the coating amount increased from 45.42 to 67.86 g/m^2. In addition, the tensile strength increased from 35.3 to 60.4 N·m/g. This indicated that the paper sheets were simultaneously endowed with excellent conductivity and tensile strength when the paper was coated with the CPU/PPy dispersion.

The conductivity stability of the conductive papers coated with different amounts of CPU/PPy was also investigated, as illustrated in Figure 14. The conductivity of the conductive paper

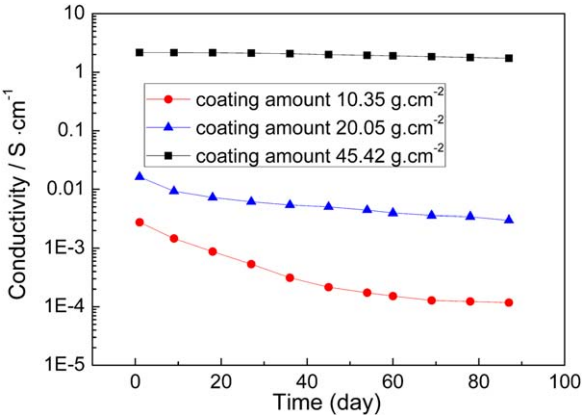

Figure 14. Conductivity stability of conductive paper coated with different amounts of CPU/PPy-20. [Color figure can be viewed in the online issue, which is available at www.interscience.wiley.com.]

coated with 10.35 g/m CPU/PPy decreased by one order after the conductive paper was stored for 87 days, although the conductivity of the conductive paper coated with 45.42 g/m^2 CPU/PPy remained almost invariable. The conductive paper sheets displayed good conductivity stability, and they may have potential applications in the fields of antistatic materials, static dissipation, and electromagnetic interference shielding.

CONCLUSIONS

Waterborne nanostructured CPU/PPy dispersions with good compatibility were successfully prepared. Good compatibility and interactions between the CPU and PPy were certified by FTIR spectroscopy, NMR, AFM, and TG–DTG, and a new chemical bond was also formed between CPU and PPy. With the introduction of PPy, the CPU/PPy colloidal particles dispersed with each other and displayed a core–shell morphology. The particle size increased from 55.08 to 74.59 nm with increasing Py content from 5 to 20 wt %, and the DPI decreased from 0.172 to 0.074. As for pure CPU, the hard-segment regions were dispersed in the soft-segment regions. The hard-segment aggregations in CPU were destroyed with the incorporation of PPy. An ordered structure with a uniform distribution of CPU and PPy was observed for the surface of the CPU/PPy films. The surface of the CPU/PPy films was covered with a smooth, coherent layer of electrically conductive PPy. When the Py content increased from 5 to 20 wt %, the conductivity of the CPU/PPy films increased from 0.1 to 5.0 S/cm. However, when the Py content was greater than 20 wt %, an apparent increase in the particle size and DPI was detected, as was the coagulation of the CPU/PPy colloidal particles; this resulted in a decreased conductivity. For the CPU/PPy-coated paper, a polymer film was developed on the top of the fibrous substrate. The surface of the conductive paper was completely enwrapped by the CPU/PPy conductive films when the coating amount was 45.42 g/m^2. With increasing coating amount from 10.35 to 67.86 g/m^2, the conductivity of the conductive coated paper increased from 2.78 $\times$ 10^{-3} to 2.16 S/cm, the tensile strength increased from 35.3 to 60.4 N m/g, and the conductive paper coated with a higher amount of CPU/PPy displayed better conductivity stability. These materials may have potential applications in the field of antistatic materials, static dissipation, and electromagnetic interference shielding.

ACKNOWLEDGMENTS

The authors express sincere thanks to the National Science Foundation of China (contract grant numbers 21204046 and 51373091), sponsorship by scientific reasearch foundation (SRF) for returned overseas chinese scholars (ROCS) and state education ministry (SEM), Shaanxi Province Science and Technology Research and Development Program of China (contract grant number 2013KJXX-77), and support by the Key Laboratory of the Education Bureau of Shaanxi Province (contract grant number 13JS018).

REFERENCES

1. Johnston, J. H.; Moraes, J.; Bommann, T. *Synth. Met.* **2005**, *153*, 65.
2. Johnston, J. H.; Kelly, F. M.; Moraes, J.; Bommann, T.; Flynn, D. *Curr. Appl. Phys.* **2006**, *6*, 587.
3. Huang, B.; Kang, G.; Ni, Y. *Can. J. Chem. Eng.* **2006**, *83*, 896.
4. Kelly, F. M.; Johhnston, J. H.; Borrmann, T.; Richardson, M. J. *Eur. J. Inorg. Chem.* **2007**, *35*, 5571.
5. Li, J.; Qian, X. R.; Chen, J. H.; Ding, C. Y.; An, X. H. *Carbohydr. Polym.* **2010**, *82*, 504.
6. Nyström, G.; Mihranyan, A.; Razaq, A.; Lindström, T.; Nyholm, L.; Strømme, M. *J. Phys. Chem. B* **2010**, *114*, 4178.
7. Wang, H. H.; Leaukosol, N.; He, Z. B.; Fei, G. Q.; Si, C. L.; Ni, Y. H. *Cellulose* **2013**, *20*, 1587.
8. Gurunathan, T.; Rao, C. R. K.; Narayan, R.; Raju, K. V. S. N. *J. Mater. Sci.* **2013**, *48*, 67.
9. Guo, Y. H.; Li, S. C.; Wang, G. S.; Ma, W.; Huang, Z. *Prog. Org. Coat.* **2012**, *74*, 248.
10. Guo, Y. H.; Guo, J. J.; Li, S. C.; Li, X.; Wang, G. S.; Huang, Z. *Colloids Surf. A* **2013**, *427*, 53.
11. Huang, X. B.; Ren, T. B.; Tian, L. Y.; Hong, L.; Zhu, W. H.; Tang, X. Z. *J. Mater. Sci.* **2004**, *39*, 1221.
12. Njuguna, J.; Pielichowski, K. *J. Mater. Sci.* **2004**, *39*, 4081.
13. Wojkiewicz, J. L.; Fauveaux, S.; Redon, N.; Miane, J. L. *Int. J. Appl. Electromagn. Mech.* **2004**, *19*, 203.
14. Reece, D. A.; Innis, S. F.; Ralph, S. F.; Wallace, G. G. *Colloids Surf. A* **2002**, *207*, 1.
15. Robilă, G.; Ivanoiu, M.; Buruiană, T.; Buruiană, E. C. *J. Appl. Polym. Sci.* **1997**, *66*, 591.
16. Robilă, G.; Diaconu, I.; Iburujană, T.; Buruiană, E.; Coman, P. *J. Appl. Polym. Sci.* **2000**, *75*, 1385.
17. Sapurina, I.; Stejskal, J.; Špírková, M.; Kotek, J.; Prokeš, J. *Synth. Met.* **2005**, *151*, 93.
18. Kotal, M.; Srivastava, S. K.; Paramanik, B. *J. Phys. Chem. C* **2011**, *115*, 1496.
19. Stejskal, J.; Sapurina, I. *Pure Appl. Chem.* **2005**, *77*, 815.
20. Somani, P. R. *Mater. Chem. Phys.* **2002**, *77*, 81.

21. Gangopadhyay, R.; De, A.; Ghosh, G. *Synth. Met.* **2011**, *123*, 21.
22. Stejskal, J.; Spirkova, M.; Riede, A.; Helmstedt, M.; Mokreva, P.; Prokes, J. *Polymer* **1999**, *40*, 2487.
23. Li, C. Y.; Chiu, W. Y.; Don, T. M. *J. Polym. Sci. Part A: Polym. Chem.* **2007**, *45*, 3902.
24. Wiersma, A. E.; Steeg, L. M. A. vd.; Jongeling, T. J. M. *Synth. Met.* **1995**, *71*, 2269.
25. Ebrahim, S.; Kashyout, A. H.; Soliman, M. *Curr. Appl. Phys.* **2009**, *9*, 448.
26. Wang, H. H.; Hu, J. J.; Shen, Y. D.; Fei, G. Q. *J. Funct. Mater.* **2013**, *44*, 689.
27. Rodrigues, P. C.; Lisboa-Filho, P. N.; Mangrich, A. S.; Akcelrud, L. *Polymer* **2005**, *46*, 2285.
28. Omastová, M.; Trchová, M.; Kovárová, J.; Stejskal, J. *Synth. Met.* **2003**, *138*, 447.
29. Carrasco, P. M.; Grande, H. J.; Cortazar, M.; Alberdi, J. M.; Areizaga, J.; Pomposo, J. A. *Synth. Met.* **2006**, *156*, 420.
30. Yang, C.; Liu, P. *Ind. Eng. Chem. Res.* **2009**, *48*, 9498.
31. Daemi, H.; Barikani, M. *Carbohydr. Polym.* **2014**, *112*, 638.
32. Zahra, M.; Zulfiqar, S.; Yavuz, C. T.; Kweon, H. S.; Sarwar, M. *Compos. Sci. Technol.* **2014**, *100*, 44.
33. Ambrozic, G.; Zigon, M. *Polym. Int.* **2005**, *54*, 606.
34. Joshi, S. D.; Vagdevi, H. M.; Vaidya, V. P.; Gadaginamath, G. S. *Eur. J. Med. Chem.* **2008**, *43*, 1989.
35. Chen, F.; Liu, P. *Macromol. Res.* **2011**, *19*, 883.
36. Chai, S. L.; Jin, M. M. *J. Appl. Polym. Sci.* **2009**, *114*, 2030.
37. Lee, J. M.; Lee, D. G.; Lee, S. J.; Kim, J. H.; Cheong, I. W. *Macromolecules* **2009**, *42*, 4511.
38. Rodrigues, P. C.; Akcelrud, L. *Polymer* **2003**, *44*, 6891.